研究論文

판재의 비드 용접에서 구속경계조건을 적용한 열응력 및 각변형 해석

배 강 열* · 최 태 완**

An Analysis of Thermal Stress and Angular Distortion in Bead-on-Plate Welding Incorporating Constrained Boundary Conditions

Kang-Yul Bae* and Tae-Wan Choi**

Key words : Bead-on-Plate Welding(판재 비드 용접), Temperature Distribution(온도분포), Thermo-elasto-plastic Analysis(열탄소성 해석), Finite Element Method(유한요소법), Two-dimensional Analysis(2차원 해석), Thermal Stress(열응력), Angular Distortion(각변형), Constrained Boundary Condition(구속경계조건)

Abstract

판재의 비드 용접과정에서 열응력과 각변형의 발생기구 및 크기를 판재 단면에 대한 2차원 유한요소해석을 통해 규명하고자 할 때, 판재의 3차원 특성을 판재 길이의 크기효과로 간주하여, 구속 경계조건으로 설정함으로써 2차원 해석으로도 더욱 실제에 근접한 현상해석이 가능함을 제안하고자 하였다

먼저 용접 입열에 의한 판재 내부의 천이 온도분포를 해석하였고, 이를 열응력 해석에 활용하였다. 2차원 열응력 해석에 있어, 용접도중에 단면 전체가 길이 방향으로 동일한 크기의 변위를 한다고 가정하여 일정 변위를 길이 방향 경계조건으로 설정하고, 판재의 길이에 따라 각변형의 발생이 구속된다고 가정하여, 판재의 길이에 의한 구속효과를 상당 구속력으로 간주하여 이를 단면 부재의 회전방향에 대한 경계조건으로 설정함으로써 판재의 3차원 특성을 고려하고자 하였다.

제안된 방법에 의한 응력 분포 형태, 각변형 크기 등의 해석 결과가 기존의 2차원 해석 결과에 비해 실제에 더 근접함을 보여 주었다

There have been many studies on the two dimensional thermo-elasto-plastic analysis in welding process, mostly from viewpoint of residual stresses. In this study, the temperature distribution, transient thermal stress, and angular distortion during bead-on-plate gas metal arc welding of rectangular plates were analyzed by using the finite element method A nonlinear heat transfer analysis was first performed by taking account of the temperature-dependent material properties and convection heat losses on the surface This was followed by a thermo-elasto-plastic stresses and distortion analysis that incorporates the constrained boundary condition of the two dimensional solution domain to get the three dimensional size effect of the plate The constrained boundary conditions adopted in this study were the constant displacement condition over the whole two dimensional section for axial movement in the welding direction, and the force boundary condition for rotational movement of the domain around the axis of the welding direction It could be revealed that the theoretical predictions of the angular distortion have an improved agreement with the experimentally obtained data presented in the previous study

× 1998년 10월 7일 접수

* 정회원, 진주산업대학교 산업자동화공학과
** 비회원, 진주산업대학교 산업자동화공학과
• 배강열 kybae@cjcc chinju ac kr

1. Introduction

The uneven temperature distribution produced during welding gives rise to incompatible strains which in turn result in distortion and self equilibrating residual stress remaining in the structure after it has cooled down to the ambient temperature. The residual stress and distortion adversely affect the service behavior of welded structures including their brittle fracture, stress corrosion cracking, fatigue and buckling characteristics In order to reduce, prevent, and/or relieve them, it is necessary to know the details of the thermal and mechanical response of weldments Therefore the prediction of the residual stress and distortion is very important

Several investigators have contributed to the solution of the welding residual stress problem in past years[1-4]. In the most of these studies, the powerful finite element method was used in the two dimensional condition, especially plane strain condition for thick plates. The predicted results and the experimental ones have been used for solving the practical problems relating to residual stress. However, it is still difficult to treat the distortion caused by welding in actual structures, because only a few primitive experimental and analytic studies are present on the two dimensional problem of the angular distortion Moreover, the analysis of welding distortion has been hindered by the difficulty of solving the problem which has a nonlinear three dimensional thermo-elasto-plastic behavior The cost of the inelastic analysis is particularly high in three dimensional calculations. Analytic studies previously performed on the angular distortion of plates have mainly used the two dimensional model with the plane strain condition in the welding direction in which the size effect of the plate can not be appropriately considered [3,4]

In this paper, a finite element model was described for analyzing the temperature, thermal stress and distortion. Particular emphasis was placed on the development of a realistic two dimensional model with constrained boundary conditions for calculating the thermal stress and angular distortion. The transient heat conduction problem was first solved, and the uncoupled thermal stress and angular distortion of the solution domain having two constrained boundary conditions were analyzed based on the calculated temperature distribution. Because the heat transfer problem can be simplified as a two dimensional one in the welding of a plate by assuming that the welding speed is sufficiently high relative to the heat conduction rate of the material, the analysis was carried out for the section of unit length located in the mid-length of the plate

The analysis of the thermal stress and angular distortion was performed on the same section having a unit length which was enforced with the constant displacement plane strain condition in the welding direction and the force boundary condition applied to the bottom of the section for compensating the size effect of the three dimensional plate. With these boundary conditions, the thermo-elasto-plastic analysis was carried out to predict the thermal stress and angular distortion of the plate in the bead-on-plate welding The material subjected to the welding thermal cycle was postulated to behave mechanically as an isotropic, elasto-plastic and strain-hardening continuum obeying the von Mises yield function and Prandtl-Reuss flow rule. The computed results of the angular distortion were then compared with the previous experimental data obtained by bead-on-plate welding of mild steel plates using the gas metal arc welding(GMAW) process[5].

2. Finite element formulation for the thermo-elasto-plastic analysis

2.1 Heat transfer analysis

The transient heat flow in a three dimensional isotropic solid bounded by a surface without internal heat generation is governed by the energy conservation equation in the Cartesian coordinate system(x,y,z) as follows.

$$-\left(\frac{\partial q_x}{\partial x}+\frac{\partial q_y}{\partial y}+\frac{\partial q_z}{\partial z}\right)=\rho c\frac{\partial T}{\partial t} \tag{1}$$

where T is the temperature, ρ the density, c the specific heat, t the time, and q_x, q_y, q_z a component of the heat flow rate vector

The weak form of eqn(1) can be derived and rearranged with integration by parts. Applying the Galerkin's method to the weak form, the governing isoparametric finite element equation of the nonlinear heat transfer problem can be written in matrix form as follows.

$$[C]\left\{\frac{dT}{dt}\right\}+[[K_c]]+[K_h]]\{T\}=\{R_q\}+\{R_h\} \tag{2}$$

The coefficient matrix $[C]$ of the time derivative of the nodal temperature is the element capacitance matrix The coefficient matrices$[K_c]$ and $[K_h]$ are the element stiffness matrices relating to the conduction and convection respectively The vectors $\{R_q\}$ and $\{R_h\}$ are the heat load vectors arising from the specified surface heating and surface convection respectively. For solving this ordinary differential equation of the nonlinear transient problem, the backward difference scheme was used in this study.

2.2 Thermo-elasto-plastic analysis

Considering the principle of virtual work for an isoparametric finite element, the equilibrium of an element at time $t+\Delta t$ can be expressed using tensor notation as follows[6].

$$\int_v {}_t^{t+\Delta t}S_{ij}\,\delta\,{}_t^{t+\Delta t}e_{ij}\,dv={}^{t+\Delta t}R \tag{3}$$

where the components of the stress S and infinitesimal strain e at time $t+\Delta t$ are referred to the configuration at time t, ${}^{t+\Delta t}R$ is the corresponding external virtual work, the subscript t denotes the reference time, the superscript $t+\Delta t$ the current time, right subscript i, j the components of the Cartesian vectors and tensors, v is the volume of an element, and δ means the variation. By incremental decompositions, the stress at time $t+\Delta t$ can be expressed as follows.

$${}_t^{t+\Delta t}S_{ij}={}^tS_{ij}+{}_tS_{ij} \tag{4}$$

where ${}^t\tau_{ij}$ is the stress component at time t, and S without left superscript indicates a finite increment. The total infinitesimal strain tensor at time $t+\Delta t$ equals the strain increment from time t because of the updated configuration and can be expressed as follows

$${}_t^{t+\Delta t}S_{ij}={}^te_{ij}=({}_tu_{i,j}+{}_tu_{j,i})/2 \tag{5}$$

where u_i is the i-th component of the displacement increment, and the comma denotes the differentiation with respect to the coordinate following.

The total strain increment is given as the summation of increments in the elastic, plastic, and thermal strain and the equivalent initial strain due to the change of the elastic property

$${}_te_{ij}={}_te_{ij}^e+{}_te_{ij}^p+{}_te_{ij}^{th}+{}_te_{ij}^{e'} \tag{6a}$$

$${}_te_{ij}^p=\Delta t\Delta^{t+\Delta t}\tau' \tag{6b}$$

$${}_te_{ij}^{th}={}^{t+\Delta t}\alpha\,{}^{t+\Delta t}T-{}^t\alpha\,{}^tT \tag{6c}$$

$${}_te_{ij}^{e'}=\frac{\partial\,[C^E]^t}{\partial T}\{{}^t\tau\}dT \tag{6d}$$

where ${}_te_{ij}^e$, ${}_te_{ij}^p$ and ${}_te_{ij}^{th}$ are the components of the elastic, plastic and thermal strain increment tensors respectively, ${}_te_{ij}^{e'}$ is the component of the equivalent initial strain tensor, α is the thermal expansion coefficient, C^E is the elastic constitutive tensor, Δ a positive constant, and τ' is the deviatoric

stress.

Then the stress increment can be expressed as follows

$$_{t}S_{ij} = {}^{t+\Delta t}C^{E}_{ijrs}({}_{t}e_{rs} - {}_{t}e^{p}_{rs} - {}_{t}e^{th}_{rs} - {}_{t}e^{o}_{rs}) \quad (7)$$

The von Mises yield function for non-isothermal, isotropic hardening was used for the calculation of Δ. With the condition that the stress-temperature state remains on the yield surface during the plastic straining and eqn(7), Δ can be obtained[7] Substituting eqn(4) and eqn(7) into eqn(3) results in the following finite element equations

$$\int_{v} B^{T} C^{E}\, _{t}e dv = -\int_{v} B^{T}\tau dv + \int_{v} B^{T} C^{E}({}_{t}e^{p} - {}_{t}e^{th} - {}_{t}e^{o})dv \quad (8)$$

where [B] is the total strain-displacement transformation matrix.

To solve the eqn(8), the modified Newton Raphson method was used. Using a difference in the strain increments between two progressive iteration steps, eqn(8) can be rewritten as follows.

$$[K]\Delta_{t}u^{(I+1)} = -\int B^{T}_{t+\Delta t} S^{(I)} dv \quad (9)$$

$${}_{t}u^{(I+1)} = {}_{t}u^{(I)} + \Delta_{t}u^{(I+1)} \quad (10)$$

$I = 0, 1, 2, \cdots$

where the stiffness matrix $[K] = \int_{v} B^{T} C B dv$, $_{t}u$ is the increment of displacement at a nodal point, and the right superscript I denotes the iteration step (I = 0 refers to the condition at time t and the iteration continues until $\Delta u \simeq 0$).

3. Process modeling and calculations

The finite element formulation performed for the thermo-elasto-plastic problem was applied to the analysis of the thermal stress and angular distortion of a plate caused by the bead-on-plate GMA welding. Figure 1(a) shows the schematic configuration of the welding process and plate

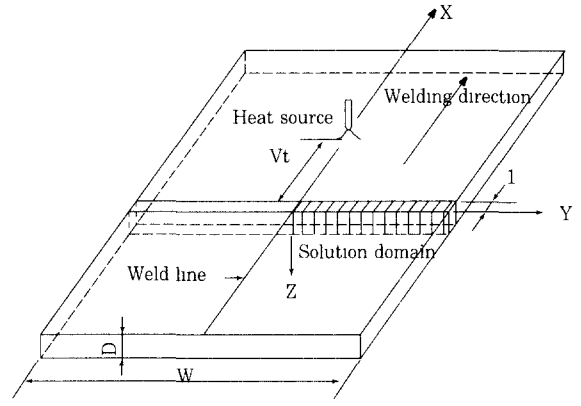

(a) Solution domain

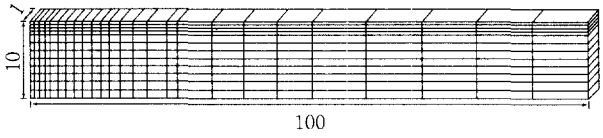

(b) Finite element mesh

Fig. 1 Solution domain and finite element mesh used for analysis of heat transfer, thermal stress and angular distortion

3.1 Heat transfer analysis

The calculation of the transient temperature distribution was based on the quasi-stationary condition, which is developed when the heat source is moving at a constant speed on a regular path, and the end effects resulting from either the initiation or termination of the heat source are neglected. This problem is, therefore, reduced to finding the two dimensional unsteady temperature field at a section normal to the weld line The two dimensional thermal analysis at the section of x=0, normal to the direction of weld line, was thus considered in the present work. The energy transfer from the arc to the workpiece top surface was simulated by the heat flux of the Gaussian distribution At other surfaces, the natural convection can be considered. At the center line of the workpiece, on which the arc moves, the temperature gradient in the transverse direction can be neglected according to the symmetry of the heat flow

3.2 Thermal stress and distortion analysis

Because of its simplicity and easiness for modeling, the plane strain boundary condition along the welding direction in weldment has been widely used for analyzing the thermal stress of the welding process However, the model using the plane boundary condition could not satisfactorily describe the thermo-mechanical behavior in the real situation except that the workpiece would be set up between two rigid constraint walls in the weld direction[8] In many real situations, however, the length of the workpiece along the longitudinal direction would be finite For predicting the thermal stress and angular distortion of the workpiece by the two dimensional analysis more realistically, the following two boundary conditions were proposed in this study.

3 2 1 Constant displacement plane strain boundary condition to the weld line

In this proposed model, the sliced solution domain was considered for calculations and its FEM mesh was as shown in Fig 1(b), where only the right half of the plate was used because of its symmetrical geometry Along the longitudinal direction one element was meshed in the solution domain to allow the change of the total strain in the welding direction Figure 2 shows the corresponding boundary condition

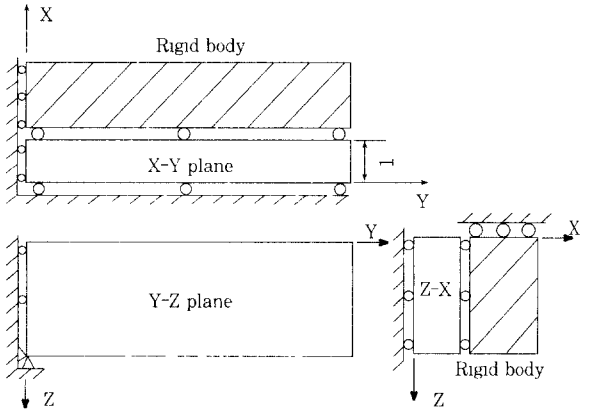

Fig. 2 Constant displacement boundary condition for analysis of thermal stress

To accept this sliced solution domain, the thermo-mechanical values were assumed to be constant along the longitudinal direction.

In this model, the distribution of the total longitudinal displacement increment u_x in the solution domain was used as the boundary condition, which can also be called plane strain condition with constant displacement[9] A real constant u_x making the resultant force along the longitudinal direction zero was considered as the boundary value. To determine u_x in the present time, an iteration procedure was needed for satisfying the following equilibrium condition in the welding direction

$$\sum F_x = 0 \tag{11}$$

3.2.2 Force boundary condition for rotational movement around weld line

In actual three-dimensional plate, angular distortion of an heated zone would be constrained by the dimensional stiffness of the other part of the plate In this study, a simplified model was proposed based on an understanding of the constraints generated by the welding process to improve the accuracy of the two dimensional distortion analysis. This model is not based on a rigorous theory, in which the force boundary condition in the form of the dimensional stiffness of the surrounding plate was applied to the bottom of the solution domain for approximating three dimensional phenomena

If the degree of constraint can be calculated for a particular section of the plate during welding, two dimensional analysis of the angular distortion is possible by adapting the dimensional stiffness as the boundary condition in the shape of the force When a fully constraining condition is enforced, the degree of the constraint can be set as $S_f = 1$

Figure 3(a) shows the location of the solution domain and heat source which starts to travel on the domain. When heat source travels on a unit length, the change of the moment(M) at the mid-section can be expected as shown in

Fig 3(b) with solid line. In this condition, the part within the length l having the positive x - directional moment behind the heat source promotes the CW distortion of the solution domain, while the other part hinders this movement Therefore, at this stage the degree of constraint S_t can be represented in the first approximation as follows

$$S_t = \frac{L-l}{L} \tag{12}$$

When x_h is less than l, i.e , the moving distance of the heat source from the solution domain is less than l, this phenomena is sustained because the length of the section $C1$ is constant and the section also moves together with the heat source.

When x_h is larger than l as shown in Fig. 3(c), the solution domain and section $A3$ start to move in the CCW direction due to cooling. To this movement, the heated region behind the solution domain makes no hindering action, because it moves in the same direction The section $A2$ having the length l is in the CW movement and the unheated section $A1$ has the stiffness effect to the movement of the domain In this case, the degree of constraint S_t can be represented as follows

$$S_t = \frac{L/2-(x_h-l)}{L/2} \quad when\ l \le x_h < l+L/2 \tag{13}$$

$$S_t = 0 \quad when\ x_h \ge l+L/2 \tag{14}$$

where, when x_h is larger than $L/2$, x_h means the elapsed time, because the welding is already ended.

In the simplified model of this study the reaction force was assumed as a dimensional stiffness of a plate enforced to a heated section For obtaining the modified stiffness in the two dimensional solution domain under a constrained condition, the reaction force at the bottom of the solution domain should vary according to the degree of constraint. Figure 3(d) shows the relationship of the reaction force between the fixed boundary condition(P_i) and the constrained case(P_i'), which can be represented as follows.

$$P_i' = P_i \ S_t \tag{15}$$

Therefore, for the analysis of the movement of the solution domain the reaction force of the fixed boundary condition at each time step should be previously determined

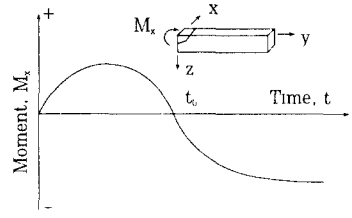

(a) Trend of angular distortion during heating of solution domain

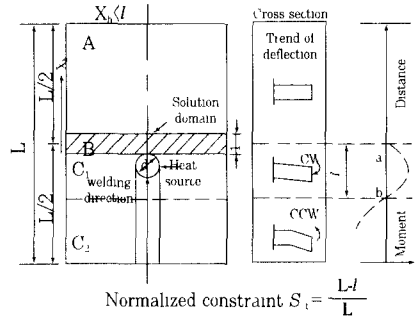

(b) Moment change at $y = 0$ section with fixed boundary condition and constrained one

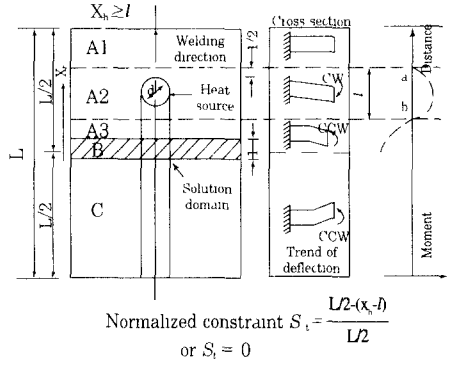

(c) Trend of angular distortion during cooling of solution domain

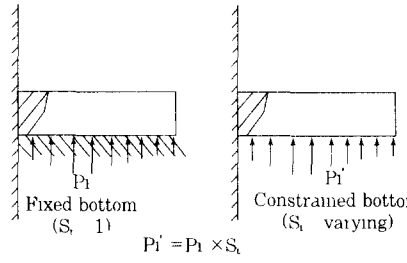

(d) Reaction force with fixed boundary condition and constrained one

Fig. 3 Conceptional drawings for force boundary condition

3.3 Material and simulation details

The incremental analysis of the thermo-elasto-plastic stress was carried out by using the finite element mesh Proper modeling of the temperature, thermal stress and angular distortion in the region close to the weld center line requires a relatively fine grid In the numerical modeling, the effective radius of arc was assumed to be 10mm, the welding speed 7mm/s, the arc efficiency 0.7, the current 281A, the voltage 31V, and the net heat input Q (=arc efficiency x heat input) 6100J/s[10] Tsuji, et al [11] showed how physical and mechanical properties of the mild steel change with the temperature. In the analysis of this study, the specific heat, the thermal conductivity, the elastic modulus, the yield strength, and the plastic modulus of the steel that change as the temperature changes were taken into account. The width of the workpiece for the simulation was 200mm, while the slice thickness was chosen to be 1mm. For acquiring the different heat input parameter(Q/D^2), 6, 8, 10, 12 and 14mm of the plate thickness were adopted. With these thickness, the heat input parameters become 16944, 9531, 6100, 4236 and 3112 J/s/cm^2 The effect of the deposited metal was neglected.

For iteratively calculating the current displacement increment($u(n+1)$), the first iteration was carried out with the displacement increment of the previous time step($u(n)$) The strain and displacement, and then the stress ($S(n+1,I)$) from the strain With these results the next displacement increment ($u(n+1, I+1)$) can be calculated at the current iteration step by the finite element equation with the modified Newton Raphson method. When the difference of displacement increment between the successive iterations ($\Delta u(I+1)$) is less than 10^{-5}, the force equilibrium was examined by enforcing a constant displacement condition in the welding direction In the finite element equation, the reaction force was included for applying the force boundary condition.

4. Results and discussion

4.1 Heat transfer analysis

Figure 4(a) shows the thermal history at several points on the surface of the 10mm thick plate heated by a Gaussian heat source The points within 5mm from the weld center line were rapidly heated up and rapidly cooled down. The point 10mm away from the weld line shows a more or less slow heating and cooling history, while the temperature level is relatively low. At the point apart larger than

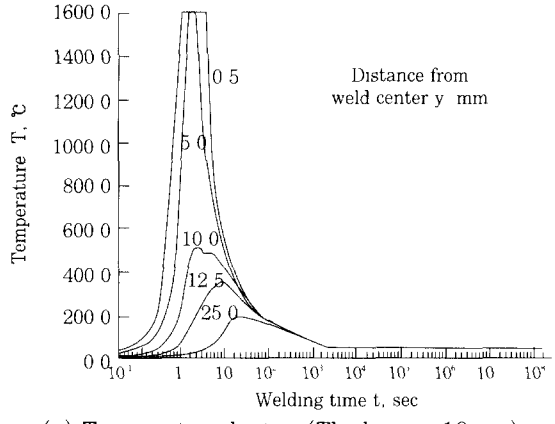

(a) Temperature history(Thickness 10mm)

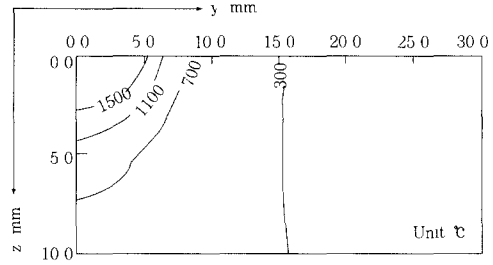

(b) Contours of maximum temperature(Thickness 10mm)

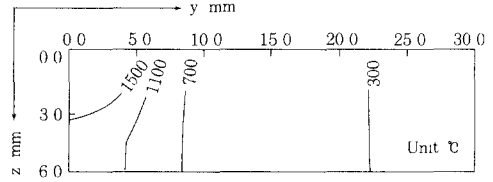

(c) Contours of maximum temperature(Thickness 6mm)

Fig. 4 Temperature history at various distance from weld center line on surface of solution domain and contours of maximum temperature

25mm, the maximum temperature was less than 200℃. This result implies that in welding the rapidly heated and cooled region occurs locally, while most of the surrounding plate is little affected by the heat source.

In Fig. 4(b), the maximum temperature occurring during the whole welding process is shown with the contour lines on the section of the solution domain In the region within about 2.8mm depth and 5.3mm width, the maximum temperature was higher than 1500℃, which would cause melting of the base plate. In the region apart more than 15mm from the heat source, the maximum temperature of 300℃ was nearly uniformly distributed along the depth direction. In Fig 4(c), when the thickness is 6mm(Heat input parameter is 16944J/s/cm^2), the melting zone becomes larger so that penetration is greater than 3mm at which the neutral axis of the plate locates. Moreover, the temperature is more evenly distributed

4.2 Thermal stress and angular distortion analysis

4.2.1 Constant displacement plane strain boundary condition to welding direction

In the thermo-elasto-plastic analysis of the thermal stress and distortion of the plate during welding, the three dimensional computation takes an awfully long time. For this reason the two dimensional analysis is widely applied with the assumption that the plate is sufficiently long to adopt the plane strain condition The result of the residual stress distribution at the top surface of the solution domain was shown with the dashed line in Fig. 5 for the plane strain condition The same result can be found in the previous study[3] With this assumption, however, the self equilibrium of the force in the welding direction can not be acquired by the section itself, and the unheated region of the plate has no strain and stress change during welding Therefore, after welding, tensile stress would be distributed over all of the heated region.

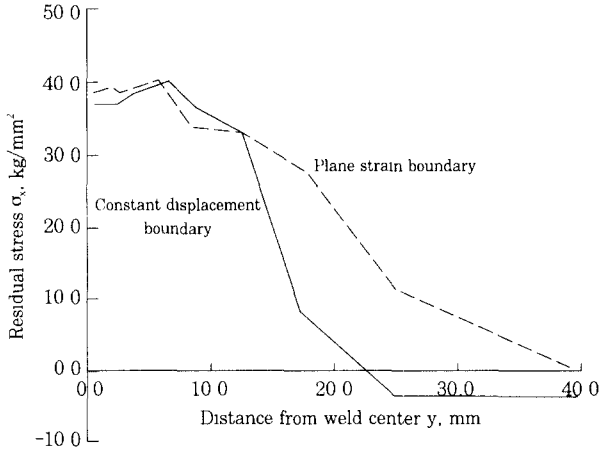

Fig. 5 Comparison of longitudinal residual stress distributions between constrained boundary and rigid one (Thickness· 10mm)

For the constrained boundary having a constant displacement in the welding direction, the residual stress distribution at the top surface of the solution domain is shown with the solid line in Fig. 5. The tensile stress was distributed around the weld line, while its maximum value was greater than the base metal yield stress with no strain hardening at room temperature. In the remaining part of the plate, to be in force equilibrium state, the small negative residual stress was distributed. This result can be considered as more realistic with respect to the previous experimental study[1]. In force balancing with the region of large tensile stress, even some part of heated region of the plate also had to have compressive stresses, and this makes much differences in the two compared results around 20mm away from weld center.

4.2.2 Force boundary condition to rotational movement around weld line

The change of the x -directional moment at $y=0$ section is shown in Fig. 6(a) versus elapsed time after welding. The moment of the constrained condition was calculated from the

moment of the fixed condition by considering the stiffness change during welding. From these results, it can be revealed that when the reverse movement occurs, the constraint becomes much smaller than in the fixed condition. Consequently there is practically no constraint to the movement of the solution domain after 11 seconds passed

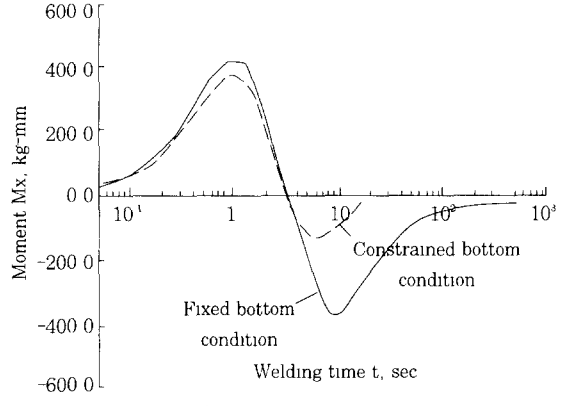

(a) Moment change

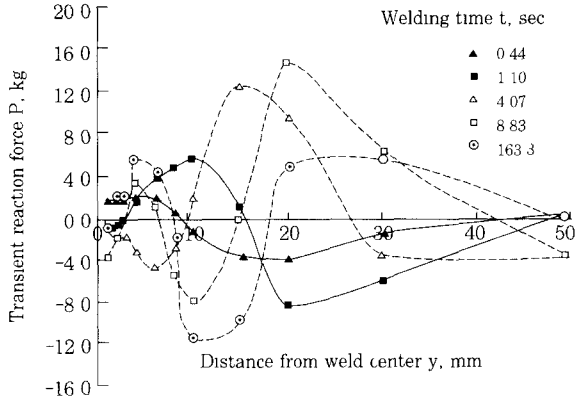

(b) Transient reaction force in fixed boundary condition

Fig. 6 Moment change at $y=0$ section and transient reaction force at bottom of domain (Thickness· 10mm)

For the solution domain fixed at the bottom surface, the reaction force against the thermal force by the welding heat source was computed along the y axis, and its result presented in Fig. 6(b). In the part near the weld center, a relatively large reaction force occurs, while its direction is reversed with the elapsed time. Small reaction force exists, if the area is more than 50mm away from the weld center, which is probably due to the fact that the displacement is absorbed mainly in the region near the weld center The reaction force was recalculated for the constrained condition by eqn[15], and this recalculated reaction force at each time step was used for the analysis of the stress and distortion.

Figure 7(a) shows the distribution change of the transient thermal stress during welding The zone of the compressive stress is broadened in the first stage of heating, but soon changed into the tensile stress state, as the highly heated part is cooled fast. However, the stress is more or less lower than that of the surrounding region and a large thermal strain would be converted to plastic strain, because the yield strength and Young's modulus are not fully recovered yet

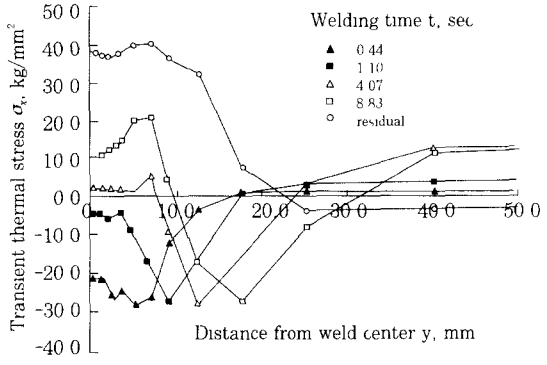

(a) Transient stress distribution

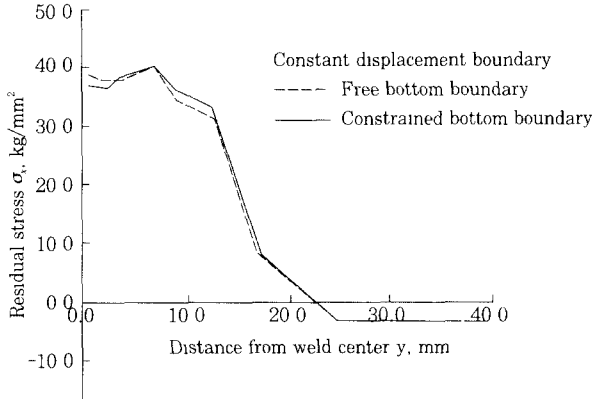

(b) Comparison of longitudinal residual stress distributions between free boundary and nstrained one

Fig. 7 Longitudinal transient and residual stress distribution(Thickness· 10mm)

The residual stress distributions at the top surface of the solution domain of the constrained and free boundary condition in the

z direction, when the domain has the constant displacement boundary condition in the x direction, are shown in Fig. 7(b). In the case of the constrained boundary condition, the maximum residual stress is somewhat different from that of the free boundary condition, which is considered to be the result of the different residual angular distortion. Contours of the equivalent plastic strain are shown in Fig 8(a),(b) for the case of the free and constrained boundary conditions respectively In the case of the constrained boundary condition, the constraining effect resulted in a little larger plastic strain.

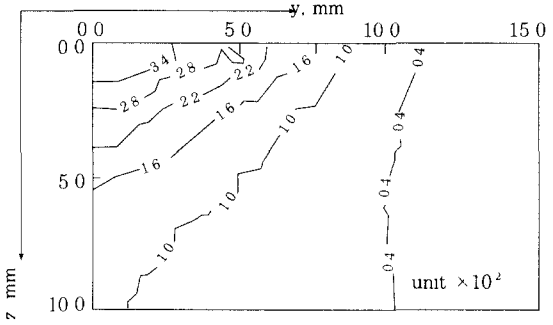

(a) For free boundary condition

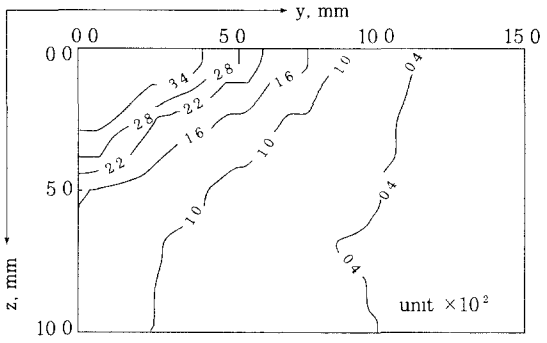

(b) For constrained boundary condition

Fig. 8 Contours of effective residual plastic strain(Thickness: 10mm)

The deflection change of the plate during welding is plotted in Fig 9(a) with the elapsed time In the case of the plane strain analysis, the solution domain can be freely deflected during heating, so that the thermal deflection is larger than that from the analysis with the constrained boundary condition. The large deflection during heating, which is recovered during cooling, results in a small value of the residual deflection, Fig 9(b)

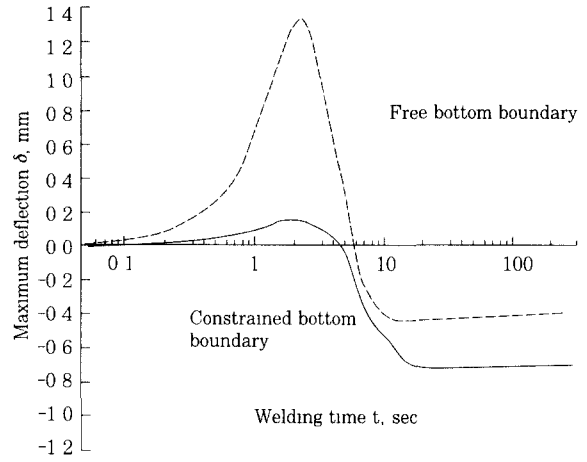

(a) Comparison of changes of maximum angular distortion between fixed boundary condition and constrained one

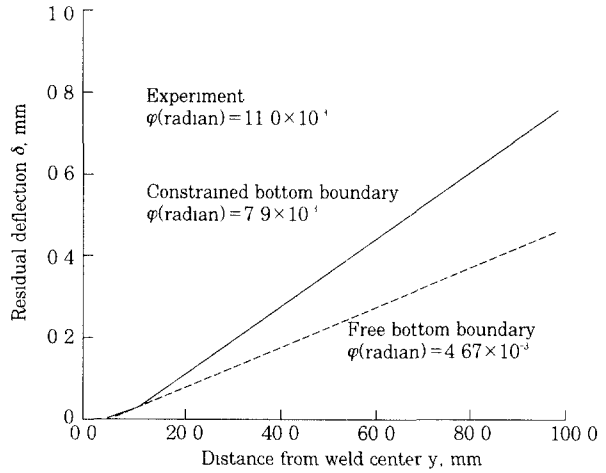

(b) Comparison of experimentally measured residual distortion with numerical predictions

Fig. 9 Changes of maximum angular distortion and residual distortion versus elapsed time (Thickness: 10mm)

With the constrained boundary condition, however, the deflection during heating is much more constrained, and consequently the final deflection is larger than that from the plane strain analysis. By comparing the calculated and experimental results, it can be revealed that the two dimensional analysis with the constrained boundary condition can predict the deflection more accurately than that with the free boundary condition. The reason why some difference exists, however, will be discussed later.

The welding distortion was calculated for

various heat input parameters and compared with the previous experimental results[5] in Fig 10

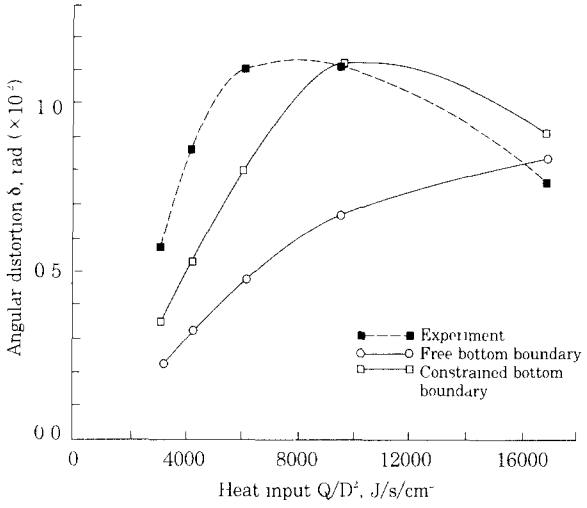

Fig. 10 Comparison of experimentally measured residual distortion with numerical prediction for various heat inputs

The predicted result for the free boundary condition showed that the residual distortion increases slowly with the increment of the heat input parameter This can be explained with Fig 9(a), in which the free boundary condition during cooling approaches its residual shape quickly, before the heat is fully conducted and consequently the temperature evenly distributed However, the actual plate in welding would constrain the section during cooling by its dimension, so that there is some time delay to achieve the residual shape of the section This phenomenon can be predicted by considering the constrained boundary conditions as shown in Fig 9(a) The angular distortion increases gradually as the heat input parameter increases, which is caused through the larger plastic strain by a larger heat input parameter However, the angular distortion decreases with increasing heat input parameter when the heat input parameter exceeds a certain value, which was considered as the result that the temperature distribution in the thickness direction becomes more even for the increasing heat input parameter. But with the free boundary condition, this phenomenon could not be obtained within the region of heat input parameter considered In this figure, however, the predicted result considering the constrained boundary still shows some difference from the experimental one This is probably due to the fact that the temperature distribution can be predicted only approximately without considering the convection effect of the molten pool in the melted zone, and also due to the non-rigorous nature of the adopted rotational boundary condition

In the comparison of the penetration profiles in GMAW acquired by calculation and experiment, the experimental result showed a deeper penetration than the predicted one by the conduction model, which could be considered as the result of the convective action of the molten pool during welding[10]. In smaller heat input parameters, for example, when the thickness is 10mm(namely, the heat input parameter is 6100J/s/cm^2), a deeper penetration in the experiment can produce a larger contraction in the upper side of the base plate, so that the residual distortion would be larger than the predicted one. By larger heat input parameters, for example, 16944J/s/cm^2 (thickness is 6mm), however, the actual penetration can be to be deeper than the neutral axis, so that the experimental residual distortion might be smaller than the predicted one Therefore, for a more accurate prediction of the angular distortion during welding, the convection of the molten pool should be considered in the calculation of the temperature distribution.

5. Conclusion

For the analysis of the thermal stress and angular distortion caused in the bead-on-plate welding, a thermo-elasto-plastic finite element analysis was performed on the two dimensional

section of the plate with the constant displacement boundary condition and the constrained boundary condition to consider the size effect of the plate. The conclusions can be summarized as follows

1) The constant displacement boundary condition in the welding direction made the two dimensional solution domain satisfy the self-equilibrium condition of the force by itself, in which the compressive longitudinal residual stress as well as the tensile stress could be produced in the base plate

2) The force boundary condition enforcing a reaction force at the bottom of the solution domain by introducing the degree of constraint enabled the two dimensional analysis to improve the accuracy of predicting the angular distortion phenomena during bead-on-plate welding

3) The residual angular distortion computed with the proposed model showed an improved agreement with the experimental one

References

1 Ueda, Y and Yamakawa, T Analysis of Thermal Elastic-Plastic Stress and Strain during Welding by Finite Element Method, Trans. of the Japan Welding Society, 1971(Vol.2), p 90-98

2. Papazoglou, V J and Masubuchi, K Numerical Analysis of Thermal Stresses during Welding including Phase Transformation Effects, Trans ASME, J Press Vessel Technol., 1982(104), p 198-203

3. Friedman, E · Thermo-mechanical Analysis of the Welding Process using the Finite Element Method, Trans ASME, J Vessel Technol , 1975(97), p.206-213

4. Argyris, J H , Szimmat, J. and Willam, K J.: Computational Aspects of Welding Stress Analysis, Computer Methods in Appl. Mech and Eng., 1982(33), p.635-666.

5. Satoh, K and Terasaki, T · Effect of Welding Conditions on Welding Deformations in Welded Structural Materials, J. Japan Welding Society, 1976(45), p 302-308.

6 Bathe, K -J : Finite Element Procedures in Engineering Analysis, 1982, Prentice-Hall, p 301-304.

7. Snyder, M.D and Bathe, K.-J A Solution Procedure for Thermo-Elasto-Plastic and Creep Problems, Nuclear Engineering and Design, 1981(64), p 49-80

8. Yang, Y.-S and Na, S -J : A Study on the Thermal and Residual Stress by Welding and Laser Surface Hardening using a New Two-dimensional Finite Element Model, Proc. Instn Mech. Engrs., Part B, 1990(204), p.167-173.

9. Sokolnikoff, I S. Mathematical Theory of Elasticity, 1978, 2nd ed , McGraw-Hill, p 250-253.

10 Kim, J.-W.: A Study on the Analysis of Weld Pool Convection and Seam Tracking by Considering the Arc Length Characteristics in GMAW, Ph.D Thesis, KAIST, 1991

11 Tsuji, I. and Yoshimura, H.· Studies on Transient Stresses and Deformation Behavior of Groove due to Butt-Welds of Thin Mild Steel Plates, J. of the Soc of Naval Architects of Japan, 1980(146), p 428-435.